DYNAMICS IN THE CENTER MANIFOLD AROUND L_2 IN THE QUASI-BICIRCULAR PROBLEM

M.A. ANDREU
Dept. Matemàtica Aplicada i Anàlisi, Univ. Barcelona,
Gran Via 585, 08007 Barcelona, Spain.
e-mail: mangel@maia.ub.es

Abstract. The Quasi-bicircular problem (QBCP) is a restricted four body problem where three masses, Earth-Moon-Sun, are revolving in a quasi-bicircular motion (that is, a coherent motion close to bicircular), the fourth mass being small and not influencing the motion of the three primaries. The QBCP is a Hamiltonian system with three degrees of freedom and depending periodically on time. The L_2 point of the QBCP is defined geometrically. It is not an equilibrium point, but there is a small periodic orbit around L_2, which has the same stability character center×center×saddle as the L_2 libration point of the restricted three body problem (RTBP). The study of orbits around L_2 can be useful for the design of future space missions. To give a full description of the different types of orbits in a neighbourhood of L_2, it is necessary to skip the hyperbolic part of the Hamiltonian. This is accomplished by the computation of the Hamiltonian reduced to the center manifold around L_2 up to high order. The methodology followed for our computations is explained in a general way so it can be applied to any other Hamiltonian system with an equilibrium point having some elliptic and some hyperbolic directions.

Keywords: Four body problem, quasi-bicircular problem, Earth-Moon-Sun system, center manifold, invariant tori.

1. Introduction

The knowledge of the dynamics around the collinear libration points of the restricted three body problem (RTBP) has been useful for the design of several space missions in the Earth-Sun system. For instance, the ISEE-3 and SOHO spacecrafts have used Halo orbits around L_1 as nominal orbits ((Farquhar et al., 1979) and (Richardson, 1980)). From these orbits it is possible to observe permanently the Sun and simultaneously to keep the communication with the Earth. Lissajous and Halo orbits around L_2 of the Earth-Sun system are also interesting. They can be used to study the geomagnetospheric tail at large distances from the Earth.

The study of the dynamics in the neighbourhood of the libration points of the Earth-Moon system is more difficult. The reason is that the RTBP is not a good model for this problem. In this case, it is necessary to take into account in some sense the influence of the Sun. To study the motion of a small particle in the Earth-Moon system several models have been used in (Mohn et al., 1967), (Kolenkiewicz et al., 1968), (Wiesel, 1984), (Gómez et al., 1987) (Scheeres et al., 1992) and (Jorba, 1999). One of the models that has been widely used is the Bicircular Problem (BCP). It considers the Earth and the Moon moving in circular orbits around their barycenter which is also moving in circular orbit around the Sun. For instance, the BCP was used in (Wiesel, 1984), (Gómez et al., 1987) and (Jorba, 1999) to study the motion near the triangular libration points of the Earth-Moon system. Nevertheless this model is not self-consistent because the movement of the three primaries is not solution of the Three Body Problem. The existence of the Sun modifies the Earth-Moon distance and therefore it can not be constant (see section 5.6.2.2 of (Szebehely, 1967)). The Quasi-bicircular problem (QBCP) is a model similar to BCP but self-consistent. This is specially important if we are interested in the motion near the L_2 point.

The QBCP has been shown to be useful for the study of the neighbourhood of the libration point L_2 of the Earth-Moon system inside the Solar system. In (Andreu et al., 1999a) and (Andreu, 1998), translunar Halo-like orbits of the real Earth-Moon system were computed from quasi-periodic Halo orbits of the QBCP. The importance of translunar Halo orbits relies on the fact that they can be used to establish a continuous communications link between the Earth and the hidden side of the Moon (Farquhar, 1970).

In section 2, we introduce the QBCP and its equations of motion. The L_2 point is not an equilibrium point but it can be defined geometrycally. Around L_2, there is a small periodic orbit having the same stability character as the corresponding point of the RTBP. It is of the form center$\times$center$\times$saddle. Some other relevant periodic orbits are also shown in that section.

Section 3 explains how to perform the reduction of the Hamiltonian to the center manifold. In this way, we skip the hyperbolic part of the Hamiltonian and get an approximation of the center manifold (Chow et al., 1982). The process of reduction to the center manifold has several steps: translation to the small periodic orbit; Floquet change of variables to diagonalize the quadratic terms of the Hamiltonian; complexification change of variables; series expansion of the terms of the potential; cancellation of suitable terms of order higher than two and realification change of variables. In our case, it is also possible to cancel the dependency on time up to high order without introducing small divisors. Then, we get the Hamiltonian reduced to the center manifold up to degree 16. That is an autonomous Hamiltonian with two degrees of freedom. We want to stress that we have implemented specific routines for the algebraic computations involved in this problem. The use of a general purpose algebraic manipulator would not be so efficient and then, probably, we would not be able to arrive up to high order in our computations.

In section 4, we make a numerical test of the accuracy of the reduced Hamiltonian. So, it is possible to know the zone where the Hamiltonian has an error smaller than a given threshold. It is important to point out that the process of reduction to the center manifold is not convergent. This is due to the fact of the accumulation of the resonances. However, the computations done show that the obtained reduced Hamiltonian is useful in a big neighbourhood around L_2. Moreover, the computation of a higher order reduced Hamiltonian would not improve the present results.

Section 5 deals with the description of the different types of orbits around L_2. For this purpose, we consider the reduced Hamiltonian restricted to several energy levels. For each energy level, a Poincaré section through an hyperplane has been used. Then, we show Poincaré sections for the most significant levels of energy. All the orbits obtained in the center manifold are interpreted in terms of the initial variables of the QBCP.

Around the L_2 point of the QBCP, there is a small periodic orbit which has characteristic of stability of the form center$\times$center$\times$saddle. Around the periodic orbit, there are families of 2D and 3D invariant tori corresponding to the center part of the dynamics. The main feature of the dynamics in the center manifold is the existence of low order (1:2) resonant periodic orbits. From these periodic orbits, several families of 2D tori emanate, which are surrounded by 3D tori. All of these are described in section 5.

Finally, some conclusions and outlook on future work are given at the end of this paper.

2. The Quasi-bicircular Problem

The Quasi-bicircular problem (QBCP) is a restricted four body problem where three masses are revolving in a quasi-bicircular motion, the fourth mass being small and not influencing the motion of the primaries. Quasi-bicircular motion means that the three primaries, P_1, P_2, P_3, are moving according to the Newton's law and if $P_{2,3}$, $P_{1,2,3}$ are the corresponding centers of masses, P_2 and P_3 around $P_{2,3}$, and P_1 and $P_{2,3}$ around $P_{1,2,3}$, are moving close to a circle. The case considered corresponds to Sun, Earth, Moon and spacecraft. The motion of the fourth mass is governed by a Hamiltonian system with three degrees of freedom and depending periodically on time.

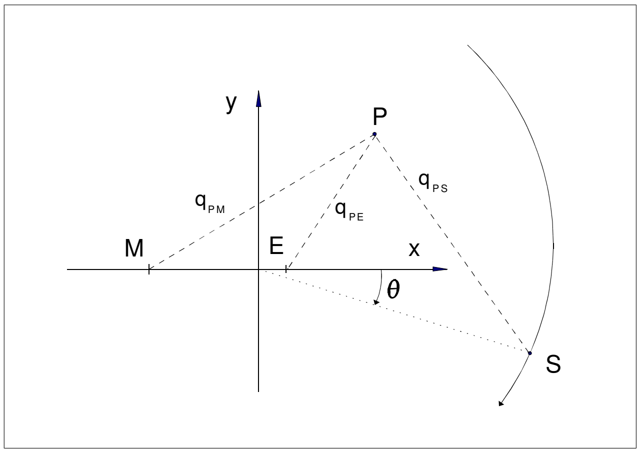

Figure 1. Geometry of the QBCP in a synodical system of reference.

The equations of the QBCP can be expressed using a synodical system of reference, this is a rotating pulsating frame centered at the Earth-Moon barycenter in such a way that the Earth and the Moon are located at fixed points $(\mu, 0, 0)$ and $(\mu - 1, 0, 0)$, respectively, where μ is the mass parameter taken as $\mu = 0.0121505816$ (see figure 1). In the synodical system, the Sun moves clockwise in a quasi-circular periodic orbit of radius $a_s = 388.81114$. Its period is denoted by T and the corresponding frequency is ω_s, which has been taken as $\omega_s = 0.925195985520347$.

The Hamiltonian of the QBCP is

$$\begin{aligned} H &= \frac{1}{2}\alpha_1(p_x^2 + p_y^2 + p_z^2) + \alpha_2(p_x x + p_y y + p_z z) + \alpha_3(p_x y - p_y x) + \\ &\quad + \alpha_4 x + \alpha_5 y - \alpha_6 \left(\frac{1-\mu}{q_{pe}} + \frac{\mu}{q_{pm}} + \frac{m_s}{q_{ps}} \right) , \end{aligned} \tag{1}$$

where

$$\begin{aligned} q_{pe}^2 &= (x-\mu)^2 + y^2 + z^2 , \\ q_{pm}^2 &= (x-\mu+1)^2 + y^2 + z^2 , \\ q_{ps}^2 &= (x-\alpha_7)^2 + (y-\alpha_8)^2 + z^2 . \end{aligned}$$

The α_k functions are of the form

$$\begin{aligned} \alpha_k(\theta) &= \alpha_{k0} + \sum_{j\geq 1} \alpha_{kj}\cos(j\theta) , \qquad \text{for } k = 1,3,4,6,7, \\ \alpha_k(\theta) &= \sum_{j\geq 1} \alpha_{kj}\sin(j\theta) , \qquad \text{for } k = 2,5,8, \end{aligned}$$

Table I. A sample of Fourier coefficients of α_k functions. All the coefficients not printed here are less than 10^{-6}.

j	α_1 c	α_2 s	α_3 c
0	1.001841608925e+00		1.000000000000e+00
1	5.767517726198e−04	−2.644376028500e−04	5.634125997554e−04
2	1.438777025508e−02	−1.328686903400e−02	1.889687440173e−02
3	−2.630362974972e−06	9.386093208090e−06	−9.911758802567e−06
4	1.176278356119e−04	−1.218509057517e−04	1.568708136031e−04
5	−8.068581391006e−08	1.522127598557e−07	−1.707762576173e−07
6	9.843249766501e−07	−1.072102664278e−06	1.319613679707e−06
j	α_4 c	α_5 s	α_6 c
0	−9.755242327485e−04		1.000907457708e+00
1	2.154764362707e+00	−2.192570751040e+00	2.870921750053e−04
2	3.657484468969e−04	−3.337210485473e−04	7.187177998613e−03
3	3.295673376167e−03	−3.295001430201e−03	−2.351183147213e−06
4	3.301031400812e−07	−3.100635053053e−07	4.585758971122e−05
5	1.278840687376e−05	−1.277777336854e−05	−3.848683620107e−08
j	α_7/a_s c	α_8/a_s s	
0	−1.623942556792e−04		
1	9.993640159328e−01	−1.002398556851e+00	
2	4.467233637764e−04	−4.460466761118e−04	
3	8.700645952865e−03	−8.707817596590e−03	
4	4.050392088510e−07	−4.001651373501e−07	
5	7.552151126648e−05	−7.555294511283e−05	

with $\theta = \omega_s t$ and the main coefficients α_{kj} are given in table I.

In chapter 2 of (Andreu, 1998) low order resonant periodic orbits around L_2 were computed. The most relevant are shown in figure 2. The small periodic orbit PO1 is, in some sense, the natural counterpart of the L_2 equilibrium point of the RTBP. We recall that L_2 in the QBCP is defined geometrically. PO2a-d are planar periodic orbits turning twice around L_2. They were computed from periodic orbits of RTBP with period $T/2$, using a continuation method. Initial points of the orbits for $t = 0$ are marked with $\circ$ or $\times$ depending on their stability character inside the center manifold. The corresponding orbit of the RTBP has been displayed with a dotted line. PO3a,c are periodic Halo orbits also turning twice around L_2. The (x, z) and (y, z) projections are shown in figure 2.

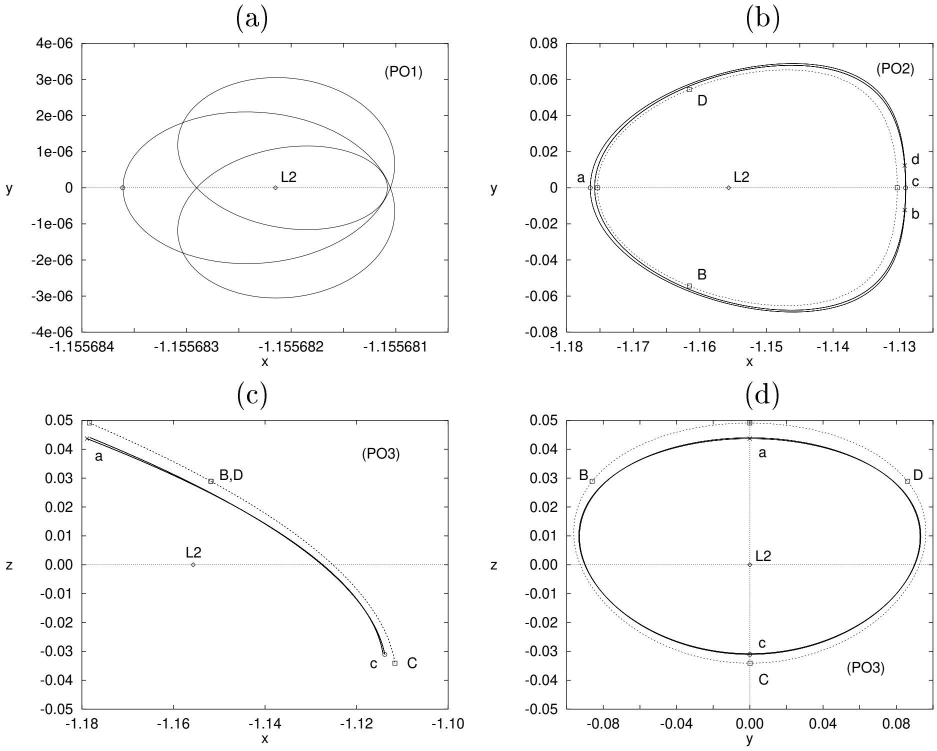

Figure 2. Periodic orbits around L_2. (a) Orbit PO1 substituting the equilibrium point. (b) Planar periodic orbits PO2a-d related to orbit of period $T/2$ of the RTBP. (c) (x, z) projection of the Halo orbits PO3a,c. (d) (y, z) projection of the previous orbits.

3. Computation of the Hamiltonian reduced to the center manifold

In the RTBP, L_2 is an equilibrium point with stability character of the form center×center×saddle. In the QBCP, the orbit PO1 inherit the same stability character of the equilibrium point of the RTBP. In order to get a description of the orbits turning around L_2, we are going to perform the reduction of the Hamiltonian of the QBCP to the center manifold. In this way, we skip the hyperbolic part of the dynamics. We want to recall that orbits around L_2 are highly unstable. Typically, for a period T (this is about 29 days) the monodromy matrix of one of this orbits has an eigenvalue of the order of 10^6.

In the next sections we are going to explain how to use Lie's method to produce a canonical change of variables from a generating function. Several of these generating functions will be computed in order to cancel the terms of degree one of the Hamiltonian, to get the normal form of the order 2 and to cancel suitable terms of order higher than 2.

3.1. Lie transformation method

Consider that our Hamiltonian is of the form

$$H = \sum_{|k|\geq 1} (\sum_j h_{kj} e^{i\,j\theta}) x^{k_1} y^{k_2} z^{k_3} p_x^{k_4} p_y^{k_5} p_z^{k_6} \ ,$$

where $h_{kj} \in \mathbb{C}$, k is the multiindex $(k_1, k_2, k_3, k_4, k_5, k_6)$ and $|k| = \sum_m k_m$. The Hamiltonian (1) can be expressed in this way expanding the potential using Legendre polynomials. However, for practical reasons, the expansion of the Hamiltonian is not computed now. It will be expanded after the computation of the Floquet change of variables.

The Hamiltonian of the QBCP has three and a half degrees of freedom, but we can consider as four degrees of freedom by introducing a new momentum y_θ, associated with the variable θ. This allows to manage time as another variable, through the angle θ. We also rename the position as $x = (x_1, x_2, x_3)$ and the momentum $y = (y_1, y_2, y_3)$. The new Hamiltonian, denoted again as H, is

$$H(x, y, \theta, y_\theta) = \omega_s y_\theta + \sum_{|k|\geq 1} H_{|k|}(x, y, \theta) \ , \tag{2}$$

where $H_{|k|}$ means terms of degree $|k|$ in x and y.

To perform canonical changes of variables, we use Lie's method (Meyer et al., 1991). Given a generating function G, the new Hamiltonian is obtained by means of

$$\tilde{H} = H + \{H, G\} + \frac{1}{2!}\{\{H, G\}, G\} + \frac{1}{3!}\{\{\{H, G\}, G\}, G\} + \dots \ ,$$

where $\{\cdot, \cdot\}$ is the Poisson bracket. For two functions, f and g, depending on (x, y, θ, y_θ), the Poisson bracket is defined as

$$\{f, g\} = \sum_{i=1}^{3} \frac{\partial f}{\partial x_i}\frac{\partial g}{\partial y_i} - \frac{\partial f}{\partial y_i}\frac{\partial g}{\partial x_i} + \frac{\partial f}{\partial \theta}\frac{\partial g}{\partial y_\theta} - \frac{\partial f}{\partial y_\theta}\frac{\partial g}{\partial \theta} \ .$$

In the particular case of a Hamiltonian of the form of (2) and a generating function G not depending on y_θ then

$$\{H, G\} = \sum_{i=1}^{3} \frac{\partial H}{\partial x_i}\frac{\partial G}{\partial y_i} - \frac{\partial H}{\partial y_i}\frac{\partial G}{\partial x_i} - \omega_s \frac{\partial G}{\partial \theta} \ .$$

The change of variables associated to the generating function G is obtained from

$$u = \tilde{u} + \{\tilde{u}, G\} + \frac{1}{2!}\{\{\tilde{u}, G\}, G\} + \frac{1}{3!}\{\{\{\tilde{u}, G\}, G\}, G\} + \dots ,$$

where u represents any of the variables and $\tilde{u}$ the corresponding new one.

3.2. Cancelling terms of degree one

The first step of the reduction to the center manifold is to cancel the terms of the Hamiltonian with degree one in x and y. That is accomplished with the translation to the periodic orbit PO1. We notice that the translation depends on time. In this way, the origin of coordinates becomes a fixed point.

For the translation to the periodic orbit, the generating function, G_1, is of the form

$$G_1 = g_{11}(\theta)x_1 + g_{12}(\theta)y_1 + g_{13}(\theta)x_2 + g_{14}(\theta)y_2 ,$$

where $g_{11}(\theta)$, $g_{12}(\theta)$, $g_{13}(\theta)$ and $g_{14}(\theta)$ are trigonometric polynomials in θ. The associated change of variables is

$$\begin{aligned} x_1 &= \tilde{x}_1 + g_{12}(\theta) , & y_1 &= \tilde{y}_1 - g_{11}(\theta) , \\ x_2 &= \tilde{x}_2 + g_{14}(\theta) , & y_2 &= \tilde{y}_2 - g_{13}(\theta) , \\ y_\theta &= \tilde{y}_\theta - \tfrac{\partial G_1}{\partial \theta} - \tfrac{1}{2}\left(g'_{11}(\theta)g_{12}(\theta) - g'_{12}(\theta)g_{11}(\theta) + \right. \\ &\qquad \left. + g'_{13}(\theta)g_{14}(\theta) - g'_{14}(\theta)g_{13}(\theta)\right) , \end{aligned}$$

where $'$ denotes the derivative. The other variables, x_3, y_3 and θ, remain unchanged. We notice that the involved periodic orbit is planar, being $x_3 = y_3 = 0$. The variable θ does not change because the function G_1 was chosen not depending on y_θ. The fact that θ remains unchanged means that the time also does not vary.

3.3. Normal form of order two

The purpose of this section is to explain how to perform a change of variables in such a way that the terms of second degree of the Hamiltonian, $H_2(x, y, \theta)$, become of the form

$$\nu_1 x_1 y_1 + \nu_2 x_2 y_2 + \nu_3 x_3 y_3 ,$$

where ν_1, ν_2 and ν_3 are constant complex numbers. This can be carried out with the use of the symplectic Floquet's theorem reducing, directly, to a diagonal form. The theorems which appear below, their proofs and the algorithm for the diagonalization of the terms of second degree of the Hamiltonian, can be found in (Gómez et al., 1993). Note that, for the application to the studied problem, the values of ν_1, ν_2 and ν_3 are $\omega_1 i$, ω_2 and $\omega_3 i$, respectively, where the ω_j will be introduced later.

Firstly, let us recall the best-known theorem of Floquet.

THEOREM 1 (Floquet). *Consider an homogeneous system of linear differential equations*

$$\dot{z} = A(t)z \, , \tag{3}$$

where $A(t)$ is a T-periodic integrable $n \times n$ matrix.

Any fundamental matrix solution $Z(t)$ of (3) *with T-periodic coefficients can be expressed in the form*

$$Z(t) = P(t)e^{Bt} \, ,$$

where $P(t)$ and B are $n \times n$ matrices, $P(t)$ is T-periodic, nonsingular for all t, and B is constant. The T-periodic change of variables $z = P(t)u$ transforms the initial system into

$$\dot{u} = Bu \, .$$

Moreover, a linear change $u = Rv$ can be applied and then the system is reduced to

$$\dot{v} = R^{-1}BRv \, .$$

The matrix R can be chosen in such a way that $R^{-1}BR$ was as simple as possible, for instance, the Jordan form of the matrix B.

We also want to remark that P satisfies the matrix differential equation

$$\dot{P} = AP - PB \, . \tag{4}$$

This equality is easily obtained differentiating $Z(t)$ and substituting into (3). The differential equation (4) will be used later on to compute $P(t)$.

For the Hamiltonian case, we have the corresponding version of the Floquet's theorem.

THEOREM 2 (Symplectic Floquet). *Let the Hamiltonian be*

$$H(X, Y, \Theta, Y_\Theta) = \omega Y_\Theta + X^T Q_1 X + X^T Q_2 Y + Y^T Q_3 Y \, , \tag{5}$$

where $Q_i = Q_i(\Theta)$ are $n \times n$ 2π-periodic matrices in the variable $\Theta = \omega t$ (say T-periodic with respect to the time t, $T = 2\pi/\omega$), and assume Q_1 and Q_3 are symmetric.

We consider the Hamiltonian equations associated with the angular variables X and their respective momenta Y:

$$\begin{array}{rcrcrl} \dot{X} &=& D_Y H &=& Q_2^T X & +2Q_3 Y \ , \\ \dot{Y} &=& -D_X H &=& -2Q_1 X & -Q_2 Y \ . \end{array}$$

We denote this system of equations by $\dot{Z} = Q(t)Z$ where $Z = (X^T, Y^T)^T$. Q is a $2n \times 2n$ T-periodic matrix with respect t and the dots denote the derivative with respect t.

Using the Floquet theorem, there exists a $2n \times 2n$ T-periodic matrix $P(t)$ such that the change of variables

$$\begin{pmatrix} X \\ Y \end{pmatrix} = \begin{pmatrix} P_{11} & P_{12} \\ P_{21} & P_{22} \end{pmatrix} \begin{pmatrix} x \\ y \end{pmatrix} ,$$

which we note $Z = Pz$, where $z = (x^T, y^T)^T$, transforms $\dot{Z} = QZ$ into $\dot{z} = Bz$, where B is a $2n \times 2n$ constant matrix which we split in four $n \times n$ matrices B_{11}, B_{12}, B_{21}, B_{22}, in the same way we do for P.

Consider the complete change of variables:

$$\begin{aligned} X &= P_{11}x + P_{12}y \ , \\ Y &= P_{21}x + P_{22}y \ , \\ \Theta &= \theta \ , \\ Y_\Theta &= y_\theta + x^T F_{11}^T x + y^T F_{12}^T x + x^T F_{21}^T y + y^T F_{22}^T y \ , \end{aligned}$$

where F_{11}, F_{12}, F_{21} and F_{22} the following $n \times n$ T-periodic matrices:

$$\begin{aligned} F_{11}^T &= \frac{-1}{2\omega} B_{21} - \frac{1}{\omega}(P_{11}^T Q_1 P_{11} + P_{11}^T Q_2 P_{21} + P_{21}^T Q_3 P_{21}) \ , \\ F_{12}^T &= \frac{1}{2\omega} B_{11} - \frac{1}{\omega}(P_{12}^T Q_1 P_{11} + P_{12}^T Q_2 P_{21} + P_{22}^T Q_3 P_{21}) \ , \\ F_{21}^T &= \frac{-1}{2\omega} B_{22} - \frac{1}{\omega}(P_{11}^T Q_1 P_{12} + P_{11}^T Q_2 P_{22} + P_{21}^T Q_3 P_{22}) \ , \\ F_{22}^T &= \frac{1}{2\omega} B_{12} - \frac{1}{\omega}(P_{12}^T Q_1 P_{12} + P_{12}^T Q_2 P_{22} + P_{22}^T Q_3 P_{22}) \ . \end{aligned}$$

Then we have:

i) The matrix B can be chosen such that it satisfies, $B^T J + JB = 0$ (it is Hamiltonian), $B_{22} = -B_{11}^T$, $B_{21} = B_{21}^T$ and $B_{12} = B_{12}^T$, where J is the symplectic matrix

$$J = \begin{pmatrix} 0 & I \\ -I & 0 \end{pmatrix} ,$$

and I is the $n \times n$ identity matrix.

ii) The complete change of variables is symplectic.

iii) The complete change of variables transforms the initial Hamiltonian $H(X, Y, \Theta, Y_\Theta)$ into

$$\tilde{H}(x, y, \theta, y_\theta) = \omega y_\theta - \frac{1}{2} x^T B_{21} x - x^T B_{22} y + \frac{1}{2} y^T B_{12} y \ .$$

3.4. The algorithm

We are going to explain the algorithm followed for the computation of the symplectic change of coordinates diagonalizing the part of second degree of the Hamiltonian of the QBCP. We notice that this change of coordinates is computed managing the initial Hamiltonian without expanding it. The expansion is performed later on.

The matrix $P(t)$ involved in the Floquet's theorem can be taken in such a way that $P(0) = I$ and so $P(T) = I$. The linearized differential equations are the variational equations. Then, integrating numerically those equations along the periodic orbit, the monodromy matrix $M = e^{BT}$ is obtained. Therefore, the matrix B is a logarithm of the matrix M divided by the period.

To get the matrix B, the next step is to compute the eigenvalues of the matrix M. Since M is a 6×6 symplectic matrix, the eigenvalues are three pairs of complex numbers λ_1, λ_1^{-1}, λ_2, λ_2^{-1}, λ_3 and λ_3^{-1}. There is a complex symplectic matrix of change of basis, S, such that $M = S D_M S^{-1}$, where D_M is the diagonal matrix

$$D_M = \left(\begin{array}{ccc|ccc} \lambda_1 & 0 & 0 & 0 & 0 & 0 \\ 0 & \lambda_2 & 0 & 0 & 0 & 0 \\ 0 & 0 & \lambda_3 & 0 & 0 & 0 \\ \hline 0 & 0 & 0 & \lambda_1^{-1} & 0 & 0 \\ 0 & 0 & 0 & 0 & \lambda_2^{-1} & 0 \\ 0 & 0 & 0 & 0 & 0 & \lambda_3^{-1} \end{array} \right) .$$

Now, the matrix B can be calculated as $B = S D_B S^{-1}$, where

$$D_B = \frac{1}{T} \log(D_M) \ .$$

It is important to remark that the complex logarithms of the elements of the diagonal of D_M are determined except by multiples of $2\pi i$. This means that we have certain freedom in choosing D_B, adding some multiple of $\omega_s i$ to any element of the diagonal of D_B and subtracting the same quantity to the conjugated element.

Although the matrices S and D_B are complex, B must be real. Then, it is also possible to express $B = RJ_BR^{-1}$, where R is a real symplectic matrix and J_B is the real Jordan form of B. The matrix R is easily obtained from S storing by columns in a suitable way the real and the imaginary parts of each complex eigenvector. In our case, the Jordan matrix is of the form

$$J_B = \left(\begin{array}{ccc|ccc} 0 & 0 & 0 & \omega_1 & 0 & 0 \\ 0 & \omega_2 & 0 & 0 & 0 & 0 \\ 0 & 0 & 0 & 0 & 0 & \omega_3 \\ \hline -\omega_1 & 0 & 0 & 0 & 0 & 0 \\ 0 & 0 & 0 & 0 & -\omega_2 & 0 \\ 0 & 0 & -\omega_3 & 0 & 0 & 0 \end{array}\right) ,$$

where we have used the values

$$\begin{aligned} \omega_1 &= 1.34709425\text{e}{-02} , \\ \omega_2 &= 2.16306748\text{e}{+00} , \\ \omega_3 &= -6.02217885\text{e}{-02} . \end{aligned} \tag{6}$$

As a consequence of the multiple determination of the complex logarithm, it would be possible to use other values of ω_1 and ω_3, adding a multiple of ω_s (we recall that $\omega_s \simeq 0.925196$). For example, in the L_2 case, we also might use

$$\begin{aligned} \bar{\omega}_1 &= \omega_1 + 2\omega_s = 1.86386291 , \\ \bar{\omega}_3 &= \omega_3 + 2\omega_s = 1.79017018 . \end{aligned} \tag{7}$$

These values coincide with the normal frequencies associated to the small periodic orbit around L_2. Moreover, they are very similar to the frequencies of the equilibrium point L_2 in the RTBP. In the next section, we will see the advantage of taking the values (6) respect to other ones.

Once the matrix B is known, it is possible to compute the matrix $P(t)$ of the Floquet's theorem by means of the matrix differential equation (4), with the initial condition $P(0) = I$. In fact, we are interested in computing $\tilde{P}(t) = P(t)R$, with the purpose that the final form of the Hamiltonian involves J_B instead of B. Then, the differential equation (4) is integrated over a period and the values of $\tilde{P}$ are stored equally spaced on time in a prefixed number of points. After, these points are used to perform an FFT obtaining a Fourier series for each component of the matrix $\tilde{P}$.

Apart from the Floquet's change of variables, the matrices F_{11}, F_{12}, F_{21} and F_{22} should also be computed. So, at the same time that $\tilde{P}$ is computed and stored, the matrices

$$F_{11}^T = \frac{-1}{2\omega_s} J_{B21} - \frac{1}{\omega_s} (\tilde{P}_{11}^T Q_1 \tilde{P}_{11} + \tilde{P}_{11}^T Q_2 \tilde{P}_{21} + \tilde{P}_{21}^T Q_3 \tilde{P}_{21}) ,$$

$$
\begin{aligned}
F_{12}^T &= \frac{1}{2\omega_s} J_{B11} - \frac{1}{\omega_s}\left(\tilde{P}_{12}^T Q_1 \tilde{P}_{11} + \tilde{P}_{12}^T Q_2 \tilde{P}_{21} + \tilde{P}_{22}^T Q_3 \tilde{P}_{21}\right) , \\
F_{21}^T &= \frac{-1}{2\omega_s} J_{B22} - \frac{1}{\omega_s}\left(\tilde{P}_{11}^T Q_1 \tilde{P}_{12} + \tilde{P}_{11}^T Q_2 \tilde{P}_{22} + \tilde{P}_{21}^T Q_3 \tilde{P}_{22}\right) , \\
F_{22}^T &= \frac{1}{2\omega_s} J_{B12} - \frac{1}{\omega_s}\left(\tilde{P}_{12}^T Q_1 \tilde{P}_{12} + \tilde{P}_{12}^T Q_2 \tilde{P}_{22} + \tilde{P}_{22}^T Q_3 \tilde{P}_{22}\right) ,
\end{aligned}
$$

are also computed and stored.

Then performing the symplectic change

$$
\begin{aligned}
X &= \tilde{P}_{11} x + \tilde{P}_{12} y , \\
Y &= \tilde{P}_{21} x + \tilde{P}_{22} y , \\
\Theta &= \theta , \\
Y_\Theta &= y_\theta + x^T F_{11}^T x + y^T F_{12}^T x + x^T F_{21}^T y + y^T F_{22}^T y,
\end{aligned}
$$

a Hamiltonian of the form (5) is transformed into

$$
\begin{aligned}
H(x, y, \theta, y_\theta) &= \omega_s y_\theta - \frac{1}{2} x^T J_{B21} x - x^T J_{B22} y + \frac{1}{2} y^T J_{B12} y = \\
&= \omega_s y_\theta + \frac{1}{2}\omega_1 (x_1^2 + y_1^2) + \omega_2 x_2 y_2 + \frac{1}{2}\omega_3 (x_3^2 + y_3^2) .
\end{aligned}
$$

Now, we introduce the canonical change of variables given by the complexification

$$
x_j = \frac{\tilde{x}_j + \tilde{y}_j\, i}{\sqrt{2}} , \qquad\qquad y_j = \frac{\tilde{x}_j\, i + \tilde{y}_j}{\sqrt{2}} ,
$$

for $j = 1, 3$, the non hyperbolic part of the Hamiltonian. In this way, the new Hamiltonian is of the form

$$
H(x, y, \theta, y_\theta) = \omega_s y_\theta + \omega_1\, i\, x_1 y_1 + \omega_2 x_2 y_2 + \omega_3\, i\, x_3 y_3 ,
$$

where we have used the same name for the new complex variables than before for the real old ones. In section 3.6, we will see that the complexification is necessary to apply an efficient algorithm to put in partial normal form terms of the Hamiltonian of order greater than two. This partial normal form allows to reduce the Hamiltonian to the center manifold and to obtain a "simplified" expression for the reduced Hamiltonian.

3.5. Expanding the Hamiltonian

We want to insist that, till now, it was not necessary to expand the Hamiltonian. The translation to the periodic orbit and the Floquet's change of variables are computed using the initial Hamiltonian. The composition of the three changes of variables (translation + Floquet + complexification) gives us another one of the form

$$\begin{aligned} z &= P(\theta)\tilde{z} + V(\theta) \, , \\ \theta &= \tilde{\theta} \, , \\ y_\theta &= \tilde{y}_\theta + \sum_{j=0}^{2} p_j(z,\theta) \, , \end{aligned} \tag{8}$$

where $z = (x_1, x_2, x_3, y_1, y_2, y_3)^T$. $P(\theta)$ is a 6×6 matrix including the Floquet's change and the complexification. Its elements are trigonometric polynomials in θ. $V(\theta)$ is the vector

$$(g_{12}, g_{14}, 0, -g_{11}, -g_{13}, 0)^T \; .$$

$p_j(z,\theta)$ are homogeneous polynomials of degree j in z and trigonometric polynomials in θ. In particular, p_0 does not depend on z and it is written as

$$p_0 = -\frac{1}{2}\left(g'_{11}(\theta)g_{12}(\theta) - g'_{12}(\theta)g_{11}(\theta) + g'_{13}(\theta)g_{14}(\theta) - g'_{14}(\theta)g_{13}(\theta)\right) \; .$$

Now, we insert the change (8) into the Hamiltonian of the QBCP. The potentials of the Earth, Moon and Sun are expanded using the recurrences involving the Legendre polynomials, but substituting the old variables by the expressions (8). We notice that this is the best way to perform the expansion. If we would have expanded the Hamiltonian at the very beginning and after we would have made the change of variables, the computational effort would be tremendous.

So, after the expansion, we get a Hamiltonian of the form

$$H(x,y,\theta,y_\theta) = \omega_s y_\theta + \omega_1\, i\, x_1 y_1 + \omega_2 x_2 y_2 + \omega_3\, i\, x_3 y_3 + \sum_{|k|\geq 3} H_{|k|}(x,y,\theta) \; ,$$

where $H_{|k|}(x,y,\theta)$ are homogeneous polynomials of degree $|k|$ in the complex variables x_1, x_2, x_3, y_1, y_2 and y_3, whose coefficients are trigonometric polynomials in θ.

3.6. Cancelling terms of order higher than two

At this point, we suppose that our Hamiltonian has the second order terms in diagonal form

$$H_2(x,y) = \omega_1 x_1 y_1 + \omega_2 x_2 y_2 + \omega_3 x_3 y_3 \; ,$$

where $\omega_j \in \mathbb{C}$, for $j = 1, 2, 3$. So, the complete Hamiltonian is

$$H(x,y,\theta,y_\theta) = \omega_s y_\theta + H_2(x,y) + \sum_{r\geq 3} H_r(x,y,\theta) \; , \tag{9}$$

with

$$H_r(x,y,\theta) = \sum_{|k|=r} h_r^k(\theta)\, x_1^{k_1} y_1^{k_2} x_2^{k_3} y_2^{k_4} x_3^{k_5} y_3^{k_6} \ ,$$

where $k = (k^1, k^2)$, with $k^1 = (k_1, k_3, k_5)$ and $k^2 = (k_2, k_4, k_6)$.

We are going to show how is possible to cancel some terms of order r of the Hamiltonian. The proposition below gives us explicitly the suitable generating function of the change of variables.

PROPOSITION 1. *Consider the Hamiltonian*

$$H = \omega_s y_\theta + H_2(x,y) + \sum_{m=3}^{r-1} H_m(x,y,\theta) + H_r(x,y,\theta) + H_{r+1}(x,y,\theta) + \cdots \ ,$$

where $r > 2$, $H_2(x,y) = \sum \omega_j x_j y_j$ $(\omega_j \in \mathbb{C}\ )$, $H_m(x,y,\theta) = \sum_{|k|=m} h_m^k(\theta) x^{k^1} y^{k^2}$, *and* $h_m^k(\theta) = \sum_j h_{m,j}^k \exp{(j\theta\, i)}$. *Let* $G_r(x,y,\theta) = \sum_{|k|=r} g_r^k(\theta) x^{k^1} y^{k^2}$ *be a generating function with*

$$g_r^k(\theta) = \sum_{j \notin\ J_k} \frac{h_{r,j}^k - \tilde{h}_{r,j}^k}{j\omega_s\, i - <\omega, k^2 - k^1>} \exp{(j\theta\, i)} \ ,$$

where $J_k = \{j \in \mathbb{Z} \ : \ j\omega_s\, i - <\omega, k^2 - k^1> = 0\}$ *and* $\omega = (\omega_1, \omega_2, \omega_3)$. *The coefficients* $\tilde{h}_{r,j}$ *are arbitrary, except for* $j \in J_k$ *for which* $\tilde{h}_{r,j} = h_{r,j}$. *Then, the new Hamiltonian* $\tilde{H}$ *obtained from* H *by means of the change of variables given by the generating function* G_r,

$$\tilde{H} = H + \{H, G_r\} + \frac{1}{2}\{\{H, G_r\}, G_r\} + \cdots \ ,$$

satisfies that

$$\tilde{H} = \omega_s y_\theta + H_2(x,y) + \sum_{m=3}^{r-1} H_m(x,y,\theta) + \tilde{H}_r(x,y,\theta) + \tilde{H}_{r+1}(x,y,\theta) + \cdots \ ,$$

where $\tilde{H}_r(x,y,\theta) = \sum_{|k|=r} \tilde{h}_r^k(\theta) x^{k^1} y^{k^2}$ *and* $\tilde{h}_r^k(\theta) = \sum_j \tilde{h}_{r,j}^k \exp{(j\theta\, i)}$.

Remarks: We notice that the terms with $j \in J_k$ are resonant terms. At this point, they can not be modified. In order to get a Hamiltonian as simple as possible, the coefficients $\tilde{h}_{r,j}^k$ (for $j \notin\ J_k$) are usually taken equal to zero. Nevertheless, when $j\omega_s\, i - <\omega, k^2 - k^1>$ is small, it is also advisable not to cancel the corresponding term. In such case, we also set $\tilde{h}_{r,j} = h_{r,j}$.

Proof. The terms of order r of the new Hamiltonian come from

$$\tilde{H}_r = H_r + \{\omega_s y_\theta, G_r\} + \{H_2, G_r\} \ .$$

By straightforward calculation we get the Poisson brackets,

$$\begin{aligned} \{\omega_s y_\theta, G_r\} &= -\omega_s \frac{\partial G_r}{\partial \theta} \ , \\ \{H_2, G_r\} &= \sum_{|k|=r} < \omega, k^2 - k^1 > g_r^k(\theta) x^{k^1} y^{k^2} \ . \end{aligned}$$

Then,

$$\tilde{H}_r = H_r - \omega_s \frac{\partial G_r}{\partial \theta} + \sum_{|k|=r} < \omega, k^2 - k^1 > g_r^k(\theta) x^{k^1} y^{k^2} \ .$$

Imposing that $\tilde{H}_r = \sum_{|k|=r} \tilde{h}_r^k(\theta) x^{k^1} y^{k^2}$, we arrive at a linear differential equation for the functions $g_r^k(\theta)$. That is

$$\omega_s \frac{dg_r^k}{d\theta} - < \omega, k^2 - k^1 > g_r^k(\theta) = h_r^k(\theta) - \tilde{h}_r^k(\theta) \ .$$

A solution of this equation is

$$g_r^k(\theta) = \sum_{j \notin \ J_k} \frac{h_{r,j}^k - \tilde{h}_{r,j}^k}{j\omega_s \, i - < \omega, k^2 - k^1 >} \exp{(j\theta \, i)} \ .$$

We notice that if $j \in J_k$ then $\tilde{h}_{r,j}^k$ must be equal to $h_{r,j}^k$ in order to avoid secular terms.

At that point, we stress that the simplicity in obtaining the generating function from the terms to be cancelled in H_r relies on the fact that we use the complexification introduced at the end of subsection 3.4. Then, in the Fourier space, the systems to be solved are diagonal.

3.7. Reduction to the center manifold

In this section, suppose that we have a Hamiltonian of the form (9), where the hyperbolic part corresponds to the variables x_2 and y_2. We recall that their exponents in the expansion have been called k_3 and k_4, respectively. To obtain the Hamiltonian reduced to the center manifold it is only necessary to cancel all the terms with $k_3 + k_4 = 1$. That is, $k_3 = 1$ and $k_4 = 0$, or $k_3 = 0$ and $k_4 = 1$. Moreover, in order to get a final Hamiltonian with the terms not depending on x_2 and y_2 as simple as possible, it would be desirable to cancel all those terms which depend on time. We also decided to cancel all the terms not depending on time, x_2 and y_2, as long as the divisor involved in the generating function was larger than 0.05. Other strategies may be used. For example, it would be possible to cancel also terms with a small divisor if the corresponding coefficient $h^k_{r,j}$ is small enough.

We notice that there is no difficulty in cancelling the terms of degree 1 in the pair x_2 and y_2. The divisor in the generating function to cancel those terms is $j\omega_s\, i \pm \omega_2$, which is always different from zero, and even more, it is never small (see the present value of ω_2 in (6)).

Concerning the terms not depending on x_2 and y_2, we discuss separately two different cases:

- Terms not depending on time: in this case, there are resonant terms which can not be cancelled. They are the ones which have $k^1 = k^2$. Apart from those terms, there are some others which can introduce small divisors in the change of variables, leading to convergence problems. For this reason, we choose the threshold $\varepsilon = 0.05$ and we kept all the terms with $< \omega, k^2 - k^1 >< \varepsilon$.

- Terms depending on time: it is very important to point out that it is possible to remove the dependency on time without introducing small divisors at low order. This is due to the fact that we choose the values of ω_1 and ω_3 as small as possible (see (6)). For instance, in the L_2 case, if we would have selected some other values like $\bar{\omega}_1$ and $\bar{\omega}_3$, then small divisors would have appeared at low order, for example, $\bar{\omega}_1 - 2\omega_s$, and so, the Hamiltonian reduced to the center manifold would depend on time. However, using the smallest values of ω_1 and ω_3, the first divisor smaller than 0.05 is $\omega_s + 15\,\omega_3$. In this way, the final Hamiltonian is autonomous up to high order.

Using the proposition 1, we can find generating functions G_3, G_4, ..., G_n to put the Hamiltonian in partial normal form up to order n. We want to point out that each change of variables G_r modifies the terms of order higher than r of the Hamiltonian. This means that before computing the next change G_{r+1}, it is necessary to transform the Hamiltonian by G_r.

Once we have the Hamiltonian in partial normal form, the center manifold is simply $x_2 = y_2 = 0$. So, the Hamiltonian reduced to the center manifold is the Hamiltonian restricted to $x_2 = y_2 = 0$. That is the terms not depending on x_2 and y_2.

In order to get the Hamiltonian in real coordinates, another change of variables must be applied. We call it *realification* and it is the inverse of the complexification done before. It is

$$
\begin{aligned}
x_j &= \frac{\tilde{x}_j - \tilde{y}_j\, i}{\sqrt{2}} \,, \\
y_j &= \frac{-\tilde{x}_j\, i + \tilde{y}_j}{\sqrt{2}} \,,
\end{aligned}
$$

for $j = 1, 3$. As usual, the variables with tilde are the new ones, but, in the following, we denote the new variables with the same name that the old ones. If all the computations done are correct, the final Hamiltonian must be real.

Using all these changes of variables, the Hamiltonian reduced to the center manifold around L_2 up to order 16 was computed. It is of the form

$$
H_{CM} = \frac{1}{2}\omega_1(x_1^2 + y_1^2) + \frac{1}{2}\omega_3(x_3^2 + y_3^2) + \sum_k h_k\, x_1^{k_1} y_1^{k_2} x_3^{k_5} y_3^{k_6} \,, \qquad (10)
$$

with $h_k \in \mathbb{R}$. Although there were some few terms leading to small divisors, they were also cancelled because their coefficients were small enough. So, with the reduction to the center manifold, we obtain an autonomous Hamiltonian.

We also computed the composition of all the changes of variables performed. We recall that they are the translation to the periodic orbit, the Floquet's change, the complexification, the changes generated by G_3, G_4, ..., G_{16} and the realification. The result is a change of variables of the form

$$
\begin{aligned}
x_j &= p_j(\tilde{x}, \tilde{y}, \theta) \,, \\
y_j &= q_j(\tilde{x}, \tilde{y}, \theta) \,, \qquad\qquad j = 1, 2, 3, \\
\theta &= \tilde{\theta} \,, \\
y_\theta &= \tilde{y}_\theta + r(\tilde{x}, \tilde{y}, \theta) \,,
\end{aligned}
$$

where p_j, q_j and r are polynomials of degree 15 in x_1, x_2, x_3, y_1, y_2 and y_3, whose coefficients are trigonometric polynomials in θ. It is a change of variables T-periodic with respect to the time. We call ψ this change of variables from coordinates of the center manifold around L_2 to the original ones of the QBCP.

4. Accuracy of the center manifold

In order to check all the computations done for the reduction to the center manifold, several tests have been implemented for different parts of the process. Here, we are going to talk about a check involving the final Hamiltonian, H_{CM}, and the initial one, H_{QBCP}.

We take an initial point in the center manifold, say $x_{cm}^{(0)}$. The Hamiltonian equations of H_{CM} are integrated with that initial condition, for a time interval of 1, for instance. Let $x_{cm}^{(1)}$ be the point obtained. The point $x_{cm}^{(0)}$ can be transformed by the change of variables ψ obtaining $x_{qbcp}^{(0)}$ in the coordinates of the QBCP. Integrating the Hamiltonian equations of H_{QBCP} for a time span of 1 with initial condition $x_{qbcp}^{(0)}$, we get $x_{qbcp}^{(1)}$. This point can be transformed by ψ^{-1} obtaining $\tilde{x}_{cm}^{(1)}$. This point is expected to be close to $x_{cm}^{(1)}$. Let d be the distance between both points, which can be considered as a function of $x_{cm}^{(0)}$.

We remind that the orbits around L_2 in the QBCP are highly unstable. If the initial conditions have some error, after the integration for a time interval of 1, that error is amplified by a factor about 10.

The distance d has been computed for several points in the center manifold along a straight line inside a level of energy. Figures 3a-c show the results for energy levels $h = 10^{-5}$, 0, -10^{-5}, along $x_1 = y_1$. Similar plots can be done for other levels of energy or using another straight lines. The tests have been done using the Hamiltonian reduced to the center manifold up to several orders. We notice that, for large orbits, the results do not improve when increasing the order. That is related to the fact that the expansions are not convergent in any open set. However, the reduction to the center manifold up to order 16 gives a good approximation of the dynamics in a neighbourhood of the libration point.

5. Description of the neighbourhood of $\mathbf{L_2}$

We would like to study the Hamiltonian restricted to the center manifold H_{CM}. In fact, we are only able to study some polynomial approximation of it. Typically, we take the approximation of order 16. When required we make comments on the approximation of other degrees. For shortness, we shall keep the name H_{CM} for the order 16 approximation. All the objects studied (say fixed points, periodic orbits, invariant manifolds, ...), should be interpreted in terms of the initial coordinates of the QBCP. From now on, the coordinates of the center manifold are called central coordinates.

The origin of the central coordinates is a fixed point that, by construction, corresponds to the small periodic orbit around L_2 (see figure 2a). However, we have found four additional fixed points in the plane $x_3 = 0$. Their coordinates and energy levels are shown in table II.

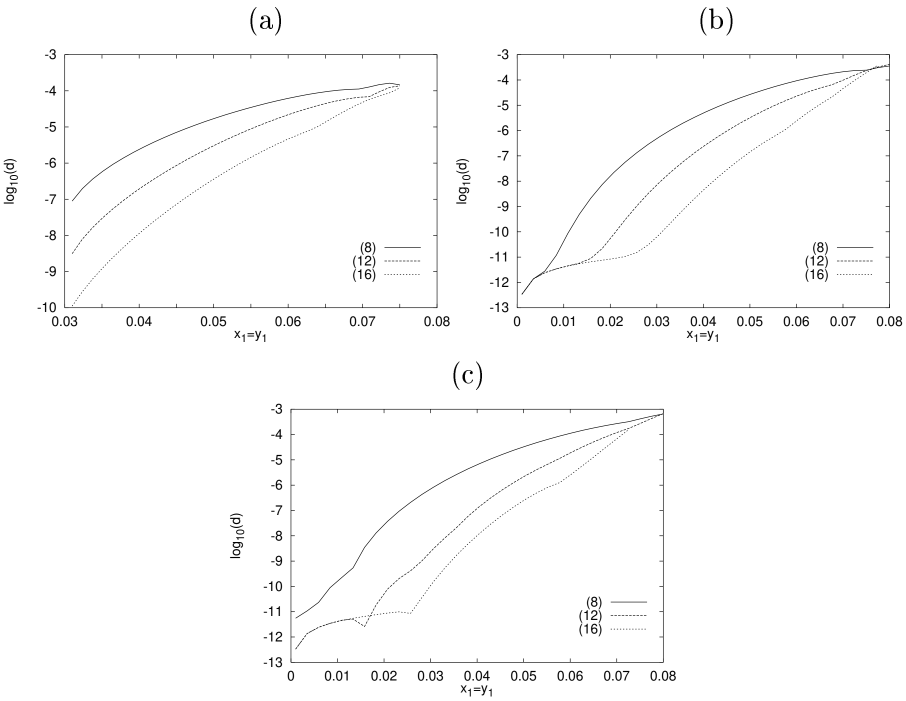

Figure 3. Results of the test of accuracy. (a) $h = 10^{-5}$, (b) $h = 0$, (c) $h = -10^{-5}$.

Table II. Fixed points of H_{CM} on the plane $x_3 = 0$. The fourth column shows the energy level $h = H_{CM}(x_1, y_1, 0, 0)$.

Label	x_1	y_1	h
2a	5.7778288e−02	5.7778292e−02	2.30211298e−05
2b	−6.6225712e−02	−4.5813575e−02	2.21256116e−05
2c	−5.6944434e−02	−5.6943907e−02	2.21256717e−05
2d	−4.5813275e−02	−6.6225920e−02	2.21256116e−05

They have been labelled with the same label that their corresponding periodic orbits PO2a-d (see figure 2b). Those periodic orbits are the ones coming from the planar Lyapunov periodic orbit of the RTBP with period $T/2$.

We want to comment that the fixed points 2a-d have the same stability character that their corresponding orbits. The points 2a and 2c are center×center. The other ones, 2b and 2d, are saddle×center. All this, of course, inside the center manifold.

Besides the fixed points on the plane $x_3 = 0$, there are another four fixed points outside of the plane. They should correspond to the

Table III. A fixed point outside the plane $x_3 = 0$ when H_{CM} is taken up to orders 12, 14 and 16.

Order	$x_1 \simeq y_1$	$x_3 \simeq y_3$
12	9.4359e−02	2.9656e−02
14	9.1658e−02	2.5544e−02
16	8.9707e−02	2.2546e−02

resonant Halo orbits of the QBCP, labelled as PO3a and PO3c (and the symmetric ones) (see figures 2a,d). But, the location of these fixed points changes a lot when considering the Hamiltonian H_{CM} up to order 12, 14 and 16. This suggests that those Halo orbits are too big and there the Hamiltonian H_{CM} does not give a good approximation of the center manifold. This agrees with the computations of the section 4. The table III shows the coordinates of one of the fixed points at different orders.

The Hamiltonian H_{CM} has two degrees of freedom, so the phase space has dimension four. For each level of energy, we can define the Poincaré map through the surface of section $\{x_3 = 0,\ \dot{x}_3 > 0\}$. This is a map defined from a two dimensional space to itself. Below, there are several figures showing some hundreds of iterations of the Poincaré map for different levels of energy.

We observe that the surface $x_3 = y_3 = 0$ is invariant for the change of variables relating the initial coordinates with the center ones. This means that the orbits living on the plane $x_3 = 0$ also lie on the plane when coming back to the initial coordinates of the QBCP. For those orbits, the Poincaré map is not defined. For higher levels of energy, it is possible to see that the boundary of the region where the Poincaré map is defined is a planar orbit on $x_3 = 0$. For lower levels of energy, the boundary is an orbit outside this plane, but then it is far away and there the Hamiltonian H_{CM} is not reliable (for more details see (Andreu, 1998)).

Figure 4a shows the Poincaré map for the level of energy $h = 2.25 \cdot 10^{-5}$, which is smaller than h_{2a}, the highest possible level of energy. In that figure, an island is seen. In the middle of the island there is a fixed point of the Poincaré map. That is a *vertical* periodic orbit of the Hamiltonian H_{CM}. Here, vertical means locally orthogonal to the plane $x_3 = 0$. Going back to the initial coordinates of the QBCP, we see that it corresponds to a 2D torus. That torus is close to the periodic orbit PO2a. In fact, we will see later that there is a family of $2D$ tori starting at the orbit PO2a. That is a resonant family of tori which is characterized by the fact that the main *horizontal* frequency is equal to $2\omega_s$. Here, horizontal means on the (x, y)-plane.

For the level h_{2a} there is only one admissible point on the Poincaré section. It corresponds, of course, to orbit of label 2a and it is located very close to center of the innermost invariant curve shown in figure 4a.

The boundary of the region where the Poincaré map of figure 4a is defined is a planar orbit. It is a periodic orbit on the plane (x_1, y_1). That is a planar 2D torus in the coordinates of the QBCP. Figure 5 shows a section of that torus. That section was obtained integrating numerically the equations of H_{CM}, taking a point of the boundary as initial condition for $t = 0$. Then, all the points with $t = 0 \pmod{T/8}$ were stored. After that, they were transformed into the initial coordinates of the QBCP. Since the main frequency of the torus is $2\omega_s$, we have four points per revolution around L_2. Those points describe four curves. Each one is homeomorphic to an $\mathbb{S}^1$. As it is natural, any slice of a 2D torus is expected to be an $\mathbb{S}^1$ (except degenerated cases).

Figure 4b corresponds to the level $h = 2.212562{\cdot}10^{-5}$. It is between h_{2c} and $h_{2b} = h_{2d}$. In the left lower part of the figure, we see a narrow island associated with the elliptic fixed point 2c. The same comments made for the island of figure 4a hold for the islands of figure 4b.

Figure 4c shows the case of $h = h_{2b} = h_{2d}$. Fixed points 2b and 2d have the same energy. In the figure, the invariant manifolds of that points have also been displayed. These manifolds are planar because they are the boundary of the region where the Poincaré map is defined for this level of energy. There is a double heteroclinic connection between the points 2b and 2d. That is, the unstable manifolds of one of them coincide with the stable manifolds of the other one. They are algebraic curves satisfying

$$H_{CM}(x_1, y_1, 0, 0) = h_{2b} = h_{2d} .$$

We recall that here H_{CM} denotes the present approximation of the Hamiltonian reduced to the center manifold, that is, a polynomial of degree 16. A “true” center manifold is, probably, at most only C^∞ and the same happens for the reduced Hamiltonian. Furthermore, because of the invariance of the $x_3 = y_3 = 0$ plane, $H_{CM}(x_1, y_1, 0, 0)$ is a Hamiltonian of one degree of freedom. This explains why an “exact” connection appears. It is difficult to appreciate the heteroclinic connection of the left lower part of figure 4c. The manifolds are very close and so, in the figure, it is not possible to see either the difference between the manifolds or the island inside.

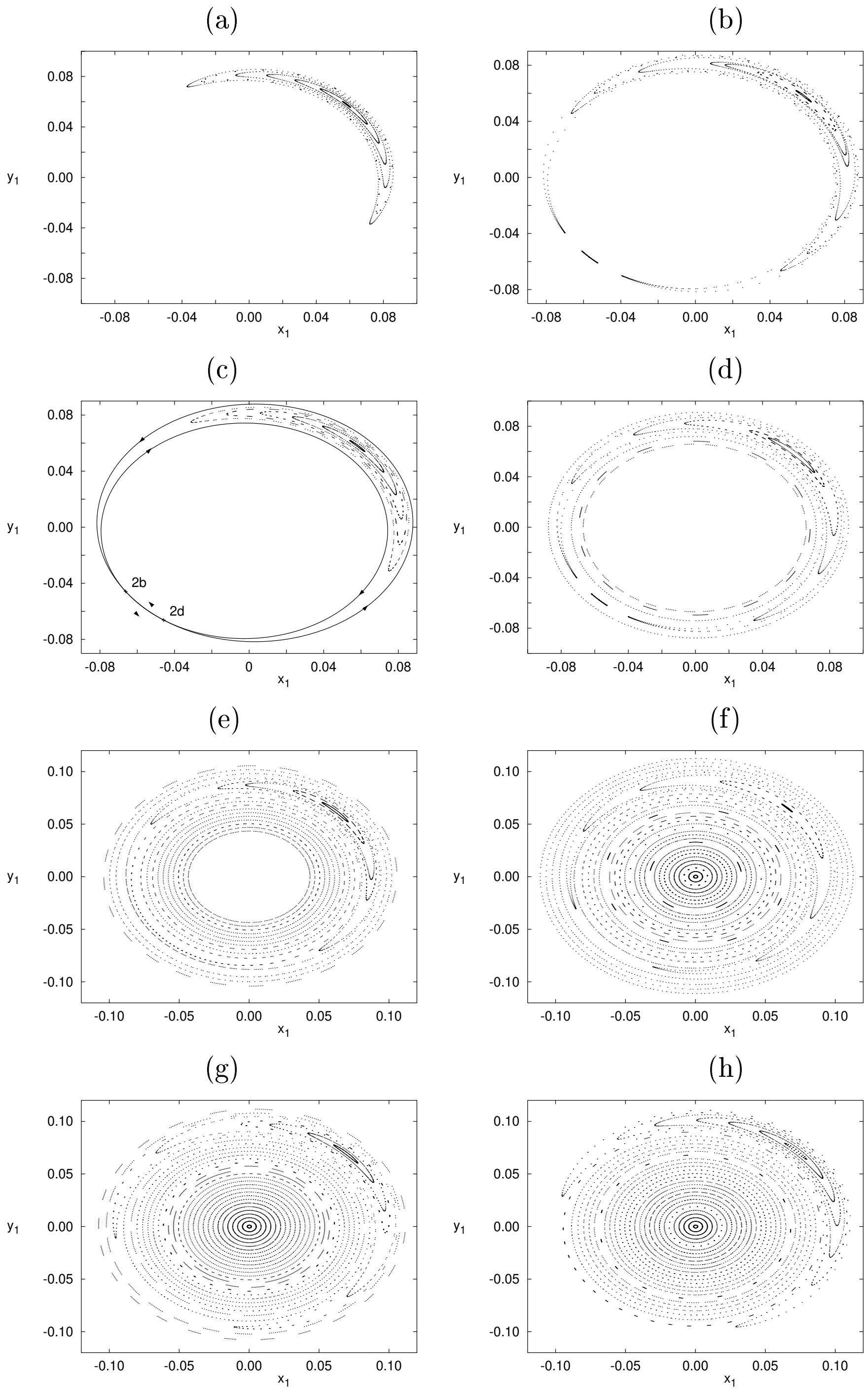

Figure 4. Poincaré map for several energy levels: (a) $h = 2.25 \cdot 10^{-5}$, (b) $h = 2.212562 \cdot 10^{-5}$, (c) $h = 2.21256116 \cdot 10^{-5}$, (d) $h = 2 \cdot 10^{-5}$, (e) $h = 10^{-5}$, (f) $h = 0$, (g) $h = -10^{-5}$, (h) $h = -1.60122 \cdot 10^{-5}$.

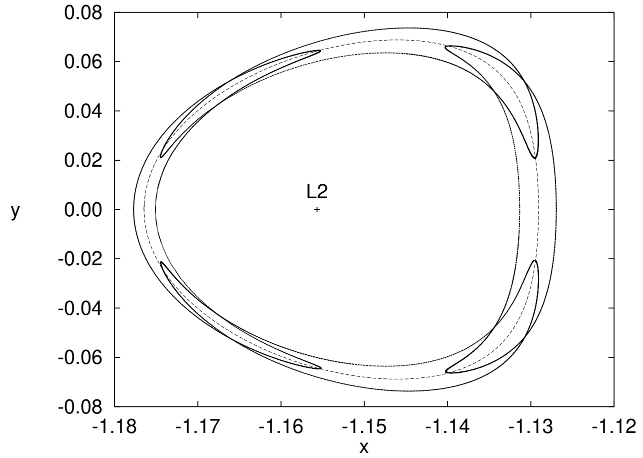

Figure 5. Section $t = 0 \pmod{T/8}$ of the boundary torus of figure 4a (QBCP coordinates). The dashed line is the periodic orbit PO2a. It has been plotted only for reference.

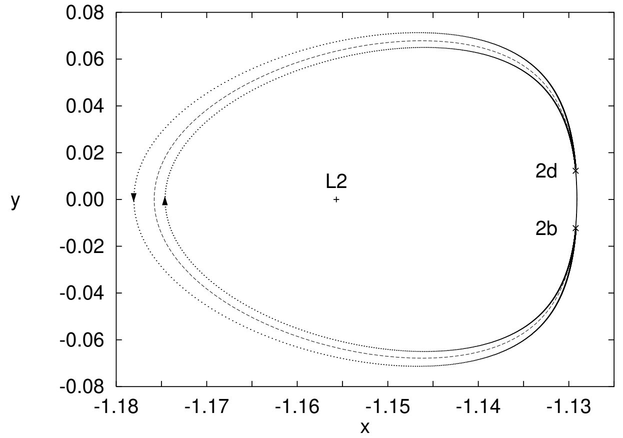

Figure 6. Invariant manifolds of the periodic orbits PO2b and PO2d, for $t = 0$ (mod T). (QBCP coordinates). The periodic orbit PO2b (dashed line) has been drawn for reference.

Now, we are interested in knowing how the previous manifolds look in the initial coordinates of the QBCP. For this purpose, we take points in the stable/unstable manifolds for $t = 0 \pmod{T}$. Those points are transformed by means of the change of variables, coming back to the initial coordinates. Figure 6 shows the resulting points. These points describe curves tending to the points of the orbits for $t = 0$. For example, in the stable manifold of the periodic orbit 2d, there are orbits rotating around L_2 in a way similar to the periodic orbit. But, the orbit in the stable manifold has a certain precession. That means that it rotates a little bit faster (or slower, depending on the branch of the stable manifold) than the periodic orbit. Therefore, looking at the orbits for instants of time spaced by the period T, the periodic orbit gives a fixed point. The orbit in the stable manifold gives a set of points tending to that fixed point.

We remark that, in the Hamiltonian H_{CM}, the invariant manifolds of the point 2b coincide with the ones of the point 2d. However, in the QBCP, probably, there is an splitting of the stable (resp. unstable) manifold of the periodic orbit 2b and the unstable (resp. stable) one of the orbit 2d. The source of this splitting relies on the lack of convergence of the reduction to the center manifold and the "autonomization" of the Hamiltonian by cancelling the dependence with respect to θ.

Figure 4d shows the Poincaré map for the level $h = 2\cdot 10^{-5}$. The region where the Poincaré map is defined is an annulus. The boundaries of this annulus are planar quasi-periodic Lyapunov orbits of the QBCP. Note that two of such orbits (the inner one and the outer one) sit in the same level of energy of H_{CM}. They have been drawn in figure 7. In that level of energy, we observe that there are four fixed points of the Poincaré map. One in the right upper part of the figure and the other three in the left lower part. Two of them are elliptic and the other two hyperbolic. We denote by $p_a(h)$, $p_b(h)$, $p_c(h)$ and $p_d(h)$ the fixed points of the Poincaré map at energy level h, related to the fixed points of H_{CM} labelled as 2a, 2b, 2c and 2d, respectively. All of these fixed points are *vertical* periodic orbits of the Hamiltonian H_{CM}. Coming back to the coordinates of the QBCP, they become 2D tori. Each of these tori belongs to a family of 2D tori which starts at one of the planar Lyapunov resonant periodic orbits (labelled also as 2a, 2b, 2c and 2d). Of course, these families are not continuous. They are supposed to be Cantor sets of 2D tori, but there is not any proof of it.

Figure 4e, corresponding to the energy level 10^{-5}, is similar to 4d, but there are two differences. One of them is evident: the "hole" of the annulus is smaller than in the previous case. We see that decreasing the value of the energy, the size of the hole is also decreasing. The other difference is that there are only two fixed points of the Poincaré map. One of them, p_a, in the upper right part of figure 4e and the other one, p_c, in the lower left part. Notice that, by decreasing the energy, the fixed points p_b, p_c and p_d have joined at a pitchfork bifurcation. This happens for the level of energy $h_{bif} = 1.707\cdot 10^{-5}$ (see figure 8). For $h > h_{bif}$, p_c is elliptic and for $h < h_{bif}$, p_c becomes hyperbolic. This means that the three families of 2D tori of the QBCP coming from periodic orbits PO2b, PO2c and PO2d join at a bifurcation and after this, only one family subsists.

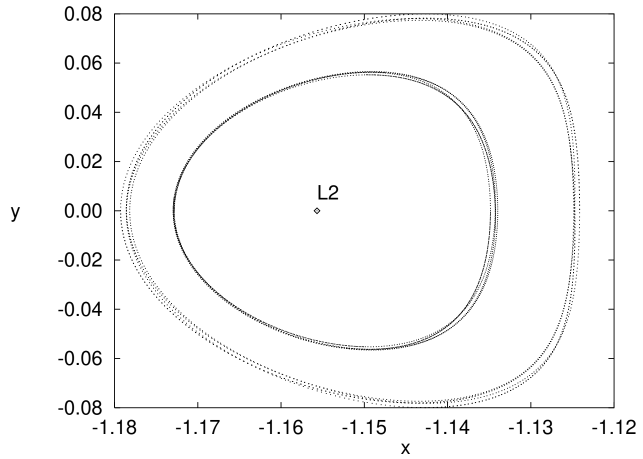

Figure 7. Planar quasi-periodic Lyapunov orbits of the boundary of the Poincaré map for $h = 2 \cdot 10^{-5}$. We have drawn the points for the time $t = kT/8$, $k = 0, \ldots, 2048$.

Figure 4f is for the value of the energy $h = 0$. This is the energy of the origin of coordinates. That point is a fixed point of the Hamiltonian H_{CM} of the type center $\times$ center. That fixed point corresponds to the small periodic orbit around L_2 (see figure 2a). From the origin, two families of 2D Lyapunov tori start. The planar one and the vertical one. We have already mentioned the planar one and we are going to talk later on about the other one.

In the RTBP, two Lyapunov families of periodic orbits emanate from the equilibrium point L_2. The results of (Jorba et al., 1997), about the persistence of lower dimensional tori under quasi-periodic perturbations, suggest that, in the QBCP, two Lyapunov families are Cantor sets of 2D tori.

Figure 4g corresponds to the level of energy $h = -10^{-5}$. It is similar to the previous one. In the top right part, as usual, there is an elliptic fixed point corresponding to a 2D torus. Several projections of that torus are shown in figure 9. In the Poincaré section, around that fixed point, there are invariant curves. Coming back to the QBCP coordinates, these curves become 3D tori around the previous 2D torus. In figure 10, we have plotted the points for the time $t = kT/8$, $k = 0, \ldots, 8192$. Since the main frequency in the xy-plane of this torus is $2\omega_s$, those points are describing four nice 2D tori. As it is natural, the section of a 3D torus looks like a 2D torus.

We have said before that, in the QBCP, a family of *vertical* quasi-periodic Lyapunov orbits starts from the orbit substituting the point L_2. In the Poincaré map, for negative values of the energy, that family

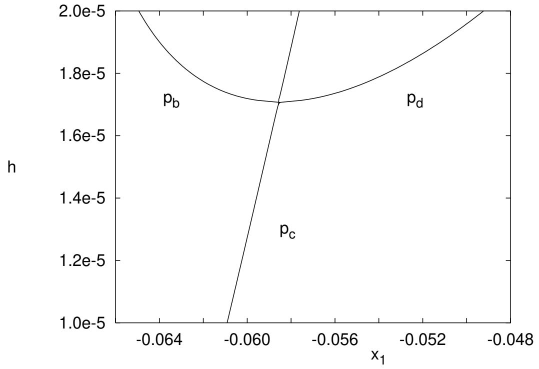

Figure 8. Bifurcation of 2D tori of the QBCP. Decreasing the energy, families of fixed points of the Poincaré maps p_b, p_c and p_d join at $h = 1.707 \cdot 10^{-5}$. After that, only the branch of p_c subsists. These fixed points correspond to the families of 2D tori related to periodic orbits PO2b, PO2c and PO2d.

of 2D tori is the origin of coordinates. That point is a fixed point of the Poincaré map. For $h = 0$, it is also a fixed point of H_{CM}. However, for negative values of the energy, it is a periodic orbit of H_{CM}. That periodic orbit becomes a 2D torus when applying the change of variables to come back to the coordinates of the QBCP. That family of 2D tori is called the *eight-shaped* family. The reason of that name is clear when looking at one of this torus. Figure 11 shows several projections of the torus corresponding to the level $h = -10^{-5}$. Note the small relative size of the scale in the y variable.

In the Poincaré map, around the origin, there are invariant curves. Generically, these curves are 3D torus of the QBCP. They are tori of the Lissajous type. Figure 12 shows one of these tori for the level of energy $h = -10^{-5}$. We have talked before about the invariant curves around fixed point p_a of the Poincaré map. They are 3D tori of the QBCP. These tori and the Lissajous tori are effectively separated by the stable and unstable manifolds of the 2D tori associated with the hyperbolic fixed points of the Poincaré map. We recall that p_b and p_d are hyperbolic for $h > h_{bif}$ and p_a is hyperbolic for $h < h_{bif}$. We note that, probably, there is an splitting between the stable and the unstable manifolds, but a particle crossing the separatrix zone would spend a very long time.

The last Poincaré section shown is at figure 4h. It is similar to the previous one. The only reason to include this figure is to notice that the island in the top right part of the figure is going farther when decreasing the energy.

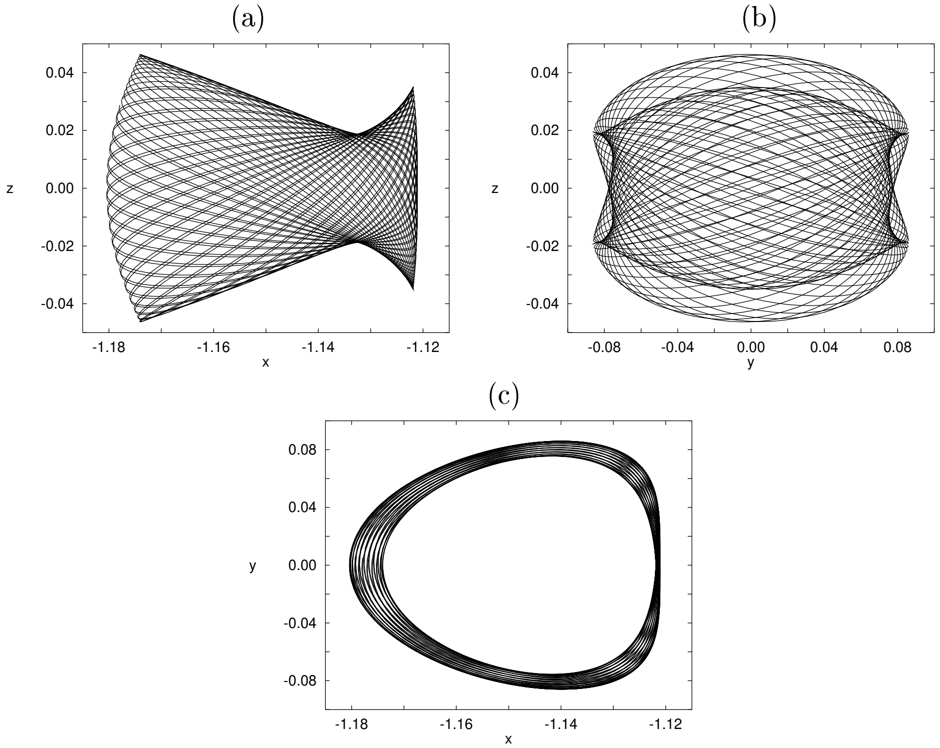

Figure 9. 2D torus corresponding to a fixed point of the Poincaré map for $h = -10^{-5}$. The orbit has been drawn for a time span of $22\,T$.

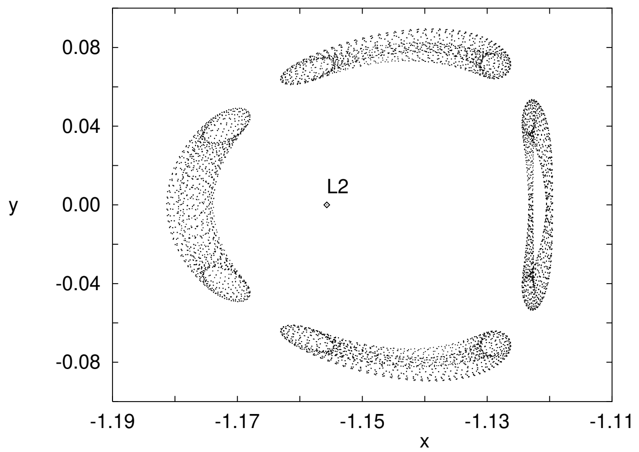

Figure 10. Section of a 3D torus around the 2D torus of figure 9. We have plotted the points for time $t = kT/8$, $k = 0, \ldots, 8192$.

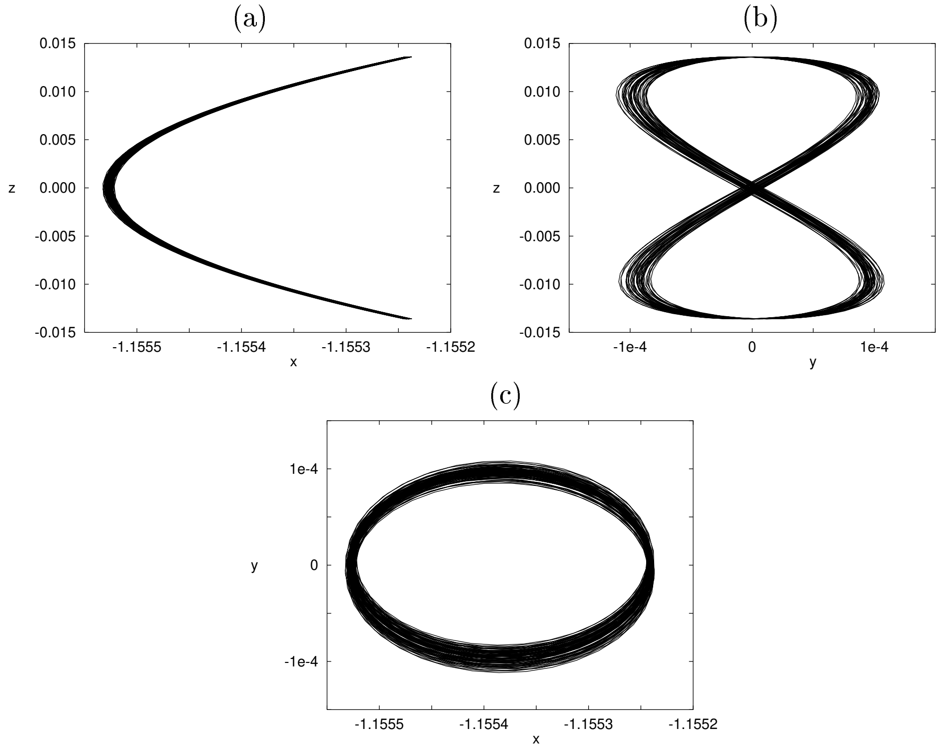

Figure 11. Eight-shaped 2D torus corresponding to the origin of coordinates of the Poincaré map for $h = -10^{-5}$. The orbit has been plotted for a time interval of $22T$.

6. Conclusion and outlook

The reduction to the center manifold allows to give a full description of the dynamics in a big neighbourhood around L_2 of the QBCP. Nevertheless, to study the Halo family of quasi-periodic orbits, it would be necessary to use a numerical method for the computation of invariant tori. This work is now in progress and some preliminary results are shown in (Andreu et al., 1999b).

7. Acknowledgements

M.A. Andreu wants to thank C. Simó for fruitful comments and suggestions about this work; J. Masdemont for providing us a lot of code which helped to implement the reduction to the center manifold; A. Delshams for reading the manuscript and suggesting several changes which improved the text. The author also wants to acknowledge the support of the catalan grant CIRIT 1998SGR-42.

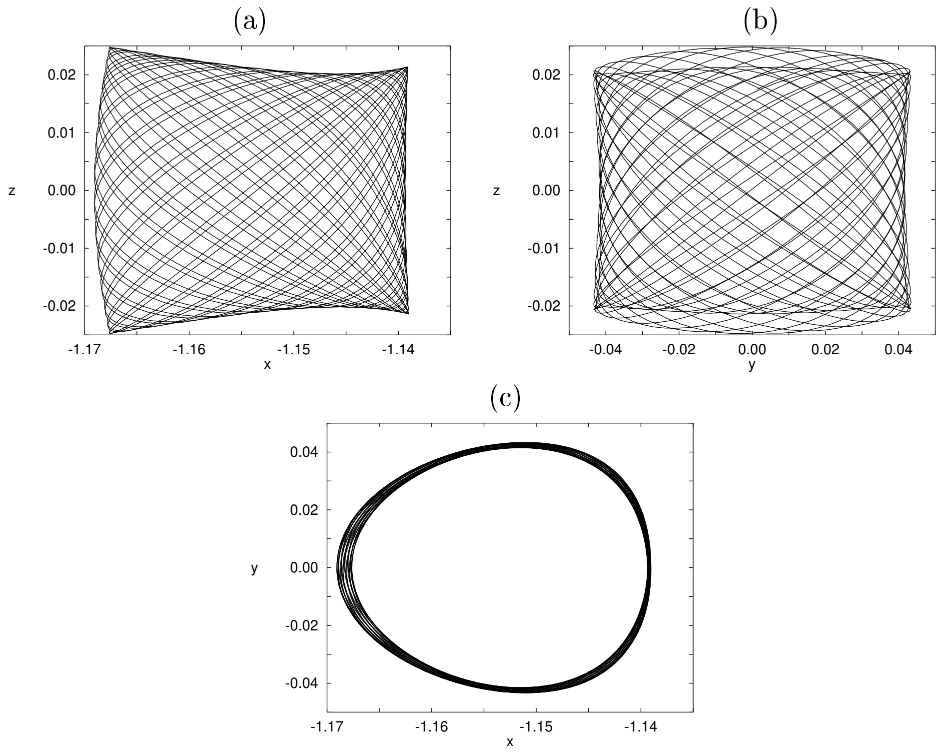

Figure 12. A 3D torus of the Lissajous type. Level of energy $h = -10^{-5}$. The orbit has been drawn for a time interval of $14\,T$.

References

Andreu, M.A.: 1998, *The Quasi-bicircular Problem*, Thesis, Dept. Matemàtica Aplicada i Anàlisi, Universitat de Barcelona.

Andreu ,M.A. and Simó, C.: 1999a, 'Translunar Halo orbits in the Quasi-bicircular Problem', B.A. Steves and A.E. Roy editors, *The Dynamics of Small Bodies in the Solar System*, NATO ASI (1997, Maratea, Italy), pp. 309-314.

Andreu, M.A. and Simó, C.: 1999b, *Estudio de la estabilidad de una familia de toros 2D del problema Cuasibicircular*, XVI CEDYA/VI CMA, (1999, Las Palmas de Gran Canaria, Spain), Vol. I, pp. 131-138.

Chow, S.N. and Hale, J.K.: 1982, *Methods of bifurcation theory*, Springer-Verlag.

Farquhar, R.W.: 1970, *The Control and Use of Libration-Point Satellites*, NASA TR R346.

Farquhar, R.W.: 1979, *The first libration point satellite, mission overview and flight history*, AAS/AIAA Astrodynamics Specialist Conference.

Gómez G., Llibre J., Martínez R. and Simó C.: 1987, *Study on orbits near the triangular libration points in the perturbed restricted three body problem*, ESOC contract 6139/84/D/JS(SC), Final Report.

Gómez G., Jorba A., Masdemont J. and Simó C.: 1993, *Study of Poincaré maps for orbits near Lagrangian points*, ESOC contract 9711/91/D/IM(SC), Final Report.

Jorba, À., Villanueva, J.: 1997, *On the persistence of lower dimensional invariant tori under quasi-periodic perturbations*, Journal of Nonlinear Science, **7** pp. 427-473.

Jorba À.: 1999, *On practical stability regions for the motion of a small particle close to the equilateral points of the real Earth-Moon system*, (preprint).

Kolenkiewicz, R. and Carpenter, L.: 1968, 'Stable periodic orbits about the Sun perturbed Earth-Moon triangular points', AIAA 6, 1301-1304.

Meyer, K.R. and Hall, G.R.: *Introduction to Hamiltonian dynamical systems and the N-body problem*, Springer-Verlag.

Mohn, L. and Kevorkian, J.: 1967, 'Some limiting case of the restricted four body problem', *Astron. Jour.* **72**, 959-963.

Richardson, D.L.: 1980, *Halo orbit formulation for the ISEE-3 mission*, J. Guidance and Control 3, pp. 543-548.

Scheeres, D.J. and Vinh, N.X.: 1992, 'The Restricted Hill Four-Body Problem', 43rd *Congress of the International Astronautical Federation*, Washington.

V. Szebehely: 1967, *Theory of orbits*, Academic Press.

Wiesel, W.: 1984, *The restricted Earth-Sun-Moon problem I: Dynamics and libration point orbits*, Dept. Aeron. and Astron., Air Force Institute of Technology Wright-Patterson AFB, Ohio.